

1 **Stacks off tracks: A role for the golgin AtCASP in plant endoplasmic**
2 **reticulum – Golgi apparatus tethering**

3

4 Anne Osterrieder^{1*}, Imogen A Sparkes^{1,2}, Stan W Botchway³, Andy Ward³, Tijs Ketelaar⁴,
5 Norbert de Ruijter⁴, Chris Hawes^{1*}

6 ¹ Department of Biological and Medical Sciences, Faculty of Health and Life Sciences,
7 Oxford Brookes University, Gypsy Lane, Headington, Oxford, OX3 0AZ, UK.

8 ² Present address: Biosciences, College of Life and Environmental Sciences, Geoffrey
9 Pope, University of Exeter, Exeter, EX4 4QD, UK

10 ³ Central Laser Facility, Science and Technology Facilities Council, Research Complex at
11 Harwell, Didcot, Oxon OX11 0FA, UK

12 ⁴ Laboratory of Cell Biology, Wageningen University, Droevendaalsesteeg 1, 6708PB
13 Wageningen, The Netherlands.

14

15 *To whom correspondence should be addressed:

16

17 Dr Anne Osterrieder
18 a.osterrieder@brookes.ac.uk
19 Tel: +44 (0)1865 4832700

20

21 Prof Chris Hawes
22 Chawes@brookes.ac.uk
23 Tel: +44 (0)1865 483266

24

25 Anne Osterrieder: a.osterrieder@brookes.ac.uk
26 Imogen A Sparkes: i.sparkes@exeter.ac.uk
27 Stan W Botchway: stan.botchway@stfc.ac.uk
28 Andy Ward: andy.ward@stfc.ac.uk
29 Tijs Ketelaar: tijs.ketelaar@wur.nl
30 Norbert de Ruijter: norbert.deruijter@wur.nl

31

32 Running title (50 chars incl spaces): Disruption of AtCASP affects ER-Golgi tethering

33 **Total word count: 5447**

34 **Highlight (29 words)**

35 Here we show that the Golgi-associated *Arabidopsis thaliana* protein AtCASP may form
36 part of a golgin-mediated tethering complex involved in anchoring plant Golgi stacks to
37 the endoplasmic reticulum (ER).

38

39 **Abstract (200 words)**

40 The plant Golgi apparatus modifies and sorts incoming proteins from the endoplasmic
41 reticulum (ER), and synthesises cell wall matrix material. Plant cells possess numerous
42 motile Golgi bodies, which are connected to the ER by yet to be identified tethering
43 factors. Previous studies indicated a role of cis-Golgi plant golgins (long coiled-coil
44 domains proteins anchored to Golgi membranes) in Golgi biogenesis. Here we show a
45 tethering role for the golgin AtCASP at the ER-Golgi interface. Using live-cell imaging,
46 Golgi body dynamics were compared in *Arabidopsis thaliana* leaf epidermal cells
47 expressing fluorescently tagged AtCASP, a truncated AtCASP- Δ CC lacking the coiled-coil
48 domains, and the Golgi marker STtmd. Golgi body speed and displacement were
49 significantly reduced in AtCASP- Δ CC lines. Using a dual-colour optical trapping system
50 and a TIRF-tweezer system, individual Golgi bodies were captured in planta. Golgi bodies
51 in AtCASP- Δ CC lines were easier to trap, and the ER-Golgi connection was more easily
52 disrupted. Occasionally, the ER tubule followed a trapped Golgi body with a gap,
53 indicating the presence of other tethering factors. Our work confirms that the intimate ER-
54 Golgi association can be disrupted or weakened by expression of truncated AtCASP- Δ CC,
55 and suggests that this connection is most likely maintained by a golgin-mediated tethering
56 complex.

57 **Keywords:** golgin, Golgi apparatus, endoplasmic reticulum, *Arabidopsis*, tethering factor,
58 secretory pathway, endomembrane system, optical tweezers.

59

60

61 **Introduction (928 words)**

62 The architecture of the Golgi apparatus is distinct and seemingly simple: An organelle
63 composed of lipids and proteins, arranged as a polarised stack of flattened cisternae,
64 capable of processing and distributing secretory cargo around and out of the cell
65 (Klumperman, 2011; Polishchuk and Mironov, 2004; Staehelin and Moore, 1995). Yet, the
66 exact mechanisms of Golgi stack assembly and maintenance are still not fully understood
67 (Wang and Seemann, 2011). It is clear though that these processes depend on a highly
68 complex and tightly regulated cascade of molecular events (Altan-Bonnet *et al.*, 2004), in
69 which proteins attach to correct membranes and precisely orchestrate a multitude of
70 tethering, fusing and budding events (Hawes *et al.*, 2010; Wilson and Ragnini-Wilson,
71 2010).

72 A Golgi stack has a *cis*-face through which it receives secretory cargo proteins from the
73 endoplasmic reticulum (ER, Hawes *et al.*, 2008; Lorente-Rodriguez and Barlowe, 2011;
74 Robinson *et al.*, 2015; Robinson *et al.*, 2007), and a *trans*-face where protein cargo exits
75 via the *trans*-Golgi network and enters intracellular or exocytotic post-Golgi transport
76 routes (Foresti and Denecke, 2008; Park and Jürgens, 2011).

77 Secretory cargo proteins move through the stack to be processed sequentially and
78 glycosylated by residential N-glycosyltransferases (Schoberer and Strasser, 2011). COPII-
79 coated membrane carriers function in anterograde ER-to-Golgi transport, whereas COPI-
80 coated vesicles transport proteins backwards within the stack and from the *cis*-Golgi stack
81 back to the ER for recycling (Robinson *et al.*, 2015).

82 To make matters more complicated, Golgi structure differs significantly between
83 kingdoms. The mammalian Golgi apparatus is most often organised as a stationary peri-
84 nuclear ‘Golgi ribbon’ in which single stacks appear to laterally fuse to create a ribbon-like
85 structure (Nakamura *et al.*, 2012). Plant cells on the other hand contain numerous discrete
86 and highly mobile Golgi bodies (Hawes and Satiat-Jeunemaitre, 2005), which move along
87 the actin cytoskeleton (Boevink *et al.*, 1998; Nebenführ *et al.*, 1999) in a myosin-dependent
88 manner (Sparkes, 2010).

89 In leaf epidermal cells, Golgi bodies and ER exit sites (specialised subdomains of the ER
90 at which protein export occurs) appear intimately associated, resulting in the adoption of
91 the “mobile secretory unit concept” (da Silva *et al.*, 2004; Hanton *et al.*, 2009; Robinson *et*
92 *al.*, 2015). A study using optical tweezers in living leaf epidermal cells confirmed this
93 concept by demonstrating a strong physical connection between ER tubules and Golgi
94 bodies upon micromanipulation of the latter (Sparkes *et al.*, 2009b).

95 However, to date we have no definite information on the nature of the molecular
96 complexes that are assumed to be involved in tethering Golgi stacks to ER exit sites. In
97 mammalian cells the golgins, a family of Golgi-localised proteins with long coiled-coil
98 domains, participate in tethering events at the Golgi (Barinaga-Rementeria Ramirez and
99 Lowe, 2009; Barr and Short, 2003; Short *et al.*, 2005; Wong and Munro, 2014). Their
100 coiled-coil domains form a rod-like structure that protrudes into the cytoplasm and thus are
101 free to interact with membranous structures such as cargo carriers and neighbouring
102 cisternae, or form a part of larger protein tethering complexes (Chia and Gleeson, 2014;
103 Gillingham and Munro, 2003; Malsam and Söllner, 2011).

104 Plants possess a set of putative golgins that locate to Golgi bodies, and protein interaction
105 partners have been identified for some of them (Gilson *et al.*, 2004; Latijnhouwers *et al.*,
106 2007; Latijnhouwers *et al.*, 2005b; Matheson *et al.*, 2007; Osterrieder, 2012; Renna *et al.*,
107 2005). Their subcellular functions largely remain unclear, although a mammalian p115
108 homologue has been suggested to be a tethering factor involved in anterograde transport
109 from the ER (Takahashi *et al.*, 2010). A *cis*-Golgi localised golgin and good candidate
110 protein for tethering Golgi bodies to ER exit sites is AtCASP (Latijnhouwers *et al.*, 2007;
111 Latijnhouwers *et al.*, 2005a; Renna *et al.*, 2005), a type II transmembrane domain protein
112 with a topology similar to the animal CASP protein (Gillingham *et al.*, 2002). Its N-
113 terminal coiled-coil domains are predicted to form a rod-like structure reaching into the
114 cytoplasm, whereas its C-terminus contains a transmembrane domain sufficient for Golgi
115 targeting (Renna *et al.*, 2005) and multiple di-acidic DXE motifs required for ER export
116 (Hanton *et al.*, 2005).

117 CASP, initially identified as a nuclear alternative splicing product of the CUTL1 gene
118 encoding the transcriptional repressor CCAAT displacement protein CDP/cut (Lievens *et*

119 *al.*, 1997), was found to locate to Golgi membranes by Gillingham and co-workers (2002).
120 The authors observed protein interactions between CASP and golgin-84 and hSec23 at
121 substoichiometric levels, as well as genetic interactions between the yeast CASP
122 homologue COY1 and the SNAREs Gos1p and Sec22p, suggesting a role for CASP in
123 membrane trafficking. Subsequently, Malsam and colleagues reported CASP to function in
124 an asymmetric tethering complex with Golgin-84, with CASP decorating Golgi
125 membranes and Golgin-84 COPI vesicles (Malsam *et al.*, 2005).

126 Our previous studies indicated a role for AtCASP in Golgi stack formation at an early
127 stage and possibly at the level of ER exit sites (Osterrieder *et al.*, 2010). After Golgi
128 membrane disruption using an inducible GTP-locked version of the small COPII GTPase
129 SAR1, GFP-AtCASP co-located with Sar1-GTP-YFP in punctate structures on the ER
130 (Osterrieder *et al.*, 2010). AtCASP also labelled reforming Golgi bodies before Golgi
131 membrane markers after washout of the secretory inhibitor Brefeldin A (Schoberer *et al.*,
132 2010).

133 In this study we used full-length and coiled-coil deletion mutant versions of AtCASP in
134 conjunction with laser tweezers (Sparkes, 2016) to assess its potential role in ER-Golgi
135 tethering and protein transport. Our findings implicate a role for AtCASP in tethering at
136 the ER-Golgi interface, as over-expression of a dominant-negative truncation interferes
137 with the stability of the ER-Golgi connection. However, our observations also suggest the
138 involvement of additional and as yet uncharacterised tethering factors.

139

140 **Materials and Methods (647 words)**

141 *Molecular biology*

142 Standard molecular techniques were used as described in Sambrook and Russel (2001).
143 Fluorescent mRFP fusions of full-length AtCASP and truncated AtCASP- Δ CC were
144 created using the previously published pENTR1A clones (Latijnhouwers *et al.*, 2007) and
145 Gateway® cloning technology according to instructions of the manufacturer (Life
146 Technologies) into the binary expression vector pB7WGR2 (Karimi *et al.*, 2002).

147 Constructs were sequenced and transformed into the *Agrobacterium tumefaciens* strain
148 GV3101::mp90

149 *Transient expression of fluorescent protein fusions in tobacco plants*

150 Transient expression of fluorescent protein fusions in tobacco leaves was carried out using
151 *Agrobacterium*-mediated infiltration of *Nicotiana tabacum* sp. lower leaf epidermal cells
152 (Sparkes *et al.*, 2006). Plants were grown in the greenhouse at 21 °C, and were used for
153 *Agrobacterium tumefaciens* infiltration at the age of 5-6 weeks. Leaf samples were
154 analysed 2–4 days after infiltration.

155 *Stable expression of Arabidopsis thaliana plants*

156 Stable *Arabidopsis* plants were created using the *Agrobacterium*-mediated floral dip
157 method (Clough and Bent, 1998). *Arabidopsis* plants from a stable GFP-HDEL line
158 (Zheng *et al.*, 2004) were transformed either with mRFP-AtCASP or mRFP-AtCASP-
159 Δ CC and grown on solid ½ MS medium with BASTA selection. All experiments were
160 performed in T3 or T4 seedlings. As control, the previously described *Arabidopsis* line
161 expressing the Golgi marker STtmd-mRFP and the ER marker GFP-HDEL was used
162 (Sparkes *et al.*, 2009b).

163 *Confocal laser scanning microscopy*

164 High-resolution confocal images were obtained using an inverted Zeiss LSM510 Meta
165 confocal laser scanning microscope (CLSM) microscope and a 40x, 63x or 100x oil
166 immersion objective. For imaging GFP in combination with mRFP, an Argon ion laser 488
167 nm and a HeNe ion laser 543 nm were used with line switching, using the multitrack
168 facility of the CLSM. Fluorescence was detected using a 488/543 dichroic beam splitter, a
169 505–530 band pass filter for GFP and a 560–615 band pass filter for mRFP.

170 *Optical trapping*

171 Optical trapping was carried out in stable *Arabidopsis* lines, using 1) a commercially
172 available dual colour system at Wageningen University, The Netherlands, comprising a
173 1063nm, 3000mW Nd:YAG laser (Spectra Physics) and x-y galvo scanner (MMI,
174 Glattbrugg, Switzerland) attached to a Zeiss Axiovert 200M with a Zeiss LSM510 Meta

175 confocal laser scanning system (Sparkes *et al.*, 2009b), and 2) a custom-built TIRF-
176 Tweezer system at the Central Laser Facility, Harwell (Gao *et al.*, 2016).

177 Golgi bodies were trapped using a 1090 nm infrared laser with intensity between 50 and
178 130 mW. For the ‘100 Golgi test’, Golgi bodies were scored as being trapped if they could
179 be moved by the laser beam.

180 *Latrunculin B treatment*

181 To inhibit actin-myosin based Golgi movement which was required during optical trapping
182 confocal microscopy, *Arabidopsis* cotyledonary leaves were treated with the actin-
183 depolymerising agent 2.5 μ M latrunculin B for 30 min as previously described (Sparkes *et*
184 *al.*, 2009b). Optical trapping experiments were performed within a time scale of two hours
185 after latrunculin B application.

186 *Tracking and statistical analysis of Golgi body and ER dynamics*

187 Movies for analysis of Golgi body dynamics in stable *Arabidopsis* lines were taken with a
188 63x PlanApo 1.4 NA oil objective at 512x512 resolution, optical zoom of 3.7 over a region
189 of interest sized 244x242 pixels, and recorded for 50 frames at 0.9 frames/sec. Individual
190 Golgi bodies were tracked using Fiji (Schindelin, *et al.* 2012) and the tracking plugin
191 MTrackJ (Meijering, *et al.* 2012). Average Golgi body displacement and speed per cell
192 were calculated from the median values using Microsoft Excel. Track lengths of trapped
193 Golgi bodies and tracks in relation to tips of ER tubules were analysed using ImageJ
194 (Schneider *et al.* 2012) and MTrackJ.

195 Statistical analysis of average displacement and speed in control and mutant cells were
196 performed in Graphpad Prism through one-way ANOVA analysis followed by unpaired
197 two-tailed type 2 Student t-tests. Statistical analysis of Golgi body trapping in control and
198 mutant lines trapped within the ‘100 Golgi test’ was performed on numerical values in
199 Microsoft Excel, using a Chi-Square test.

200

201

202 **Results (2217 words)**

203 *Fluorescently labelled full-length and mutant AtCASP constructs co-locate with the Golgi*
204 *marker STtmd-GFP in tobacco leaf epidermal cells*

205 The first step in assessing the function of a putative protein tether is to disturb its tethering
206 capability. If AtCASP played a role in tethering events between the ER and Golgi bodies,
207 deleting its coiled-coil domain could be predicted to affect Golgi morphology, function or
208 dynamics, possibly resulting in changes in: 1) the subcellular location of the fluorescent
209 mutant compared to the full-length protein, 2) the subcellular location of Golgi bodies in
210 relation to the endoplasmic reticulum, 3) Golgi body dynamics, such as speed or
211 displacement, or 4) in the physical interaction between Golgi bodies and the endoplasmic
212 reticulum tested by optical tweezer based displacement of Golgi bodies.

213 The mRFP (monomeric red fluorescent protein) constructs used for this study were full-
214 length AtCASP and a deletion mutant AtCASP- Δ CC. In this mutant, the coiled-coil
215 domains were deleted to produce a truncated protein. AtCASP- Δ CC consists of the C-
216 terminal 463 base pairs, including a transmembrane domain that confers Golgi localisation
217 (Figure 1a, Latijnhouwers *et al.*, 2007; Renna *et al.*, 2005). This construct may act as a
218 dominant-negative mutant, as it competes with endogenous wild type AtCASP for Golgi
219 membrane insertion, but lacks the native protein's potential tethering functions. As
220 previously described for the green fluorescent protein (GFP) versions (Latijnhouwers *et*
221 *al.*, 2007; Renna *et al.*, 2005), upon transient expression in tobacco leaf epidermal cells,
222 the full-length mRFP-AtCASP co-located with the standard Golgi marker STtmd-GFP
223 (Boevink *et al.*, 1998) in punctate structures (Figure 1b). Similarly, mRFP-AtCASP- Δ CC
224 contained sufficient information to target the fluorescent fusion protein to Golgi bodies
225 (Figure 1c). No obvious changes in localization were observed between the full-length and
226 the mutant AtCASP construct.

227

228 *Golgi body speed and displacement are significantly reduced in mutant AtCASP lines*

229 To obtain qualitative and quantitative data on any changes in interactions between Golgi
230 bodies and the ER, stable *Arabidopsis* lines expressing full-length mRFP-AtCASP or

231 mRFP-AtCASP- Δ CC in a GFP-HDEL background were created. A transgenic *Arabidopsis*
232 line expressing the Golgi marker STmd-mRFP and the ER marker GFP-HDEL (Runions
233 *et al.*, 2006; Sparkes *et al.*, 2009b) was used as a control (Figure 2a). Cotyledonary leaf
234 epidermal cells in 4-6 day old seedlings were analysed using confocal laser scanning
235 microscopy. Neither the mRFP-AtCASP/GFP-HDEL lines (Figure 2b) nor the mutant
236 mRFP-AtCASP- Δ CC/GFP-HDEL lines (Figure 2c) displayed any obvious differences, at
237 the resolution of the confocal microscope, in Golgi morphology, or spatial positioning
238 relative to the surface of the ER, compared to the control.

239 To obtain quantitative data, movies were taken from control, full-length and mutant
240 epidermal leaf cells and analysed using automated particle tracking software. Golgi bodies
241 in mRFP-AtCASP lines formed clusters or chains, often just temporary in nature, with
242 clusters dissolving after a few seconds and individual Golgi bodies continuing to move
243 along their single trajectories (Figure 2b). Golgi body movement was therefore analysed
244 manually using the MTrackJ plugin (Meijering *et al.*, 2012) in the ImageJ processing
245 package Fiji (Schindelin *et al.*, 2012). MtrackJ allows the manual tracking of individual
246 Golgi bodies frame by frame and the software was used to determine the mean speed and
247 displacement (the straight line distance from the start point of the track to the current point
248 measure, abbreviated here as D2S) for individual Golgi bodies in control, full-length and
249 mutant AtCASP lines.

250 Mean Golgi body speed and displacement were calculated from the pooled Golgi body
251 data (n ranging between 3-19 Golgi bodies per cell). Table 1 summarises the number of
252 individual lines, cells and Golgi bodies that were analysed. All Golgi body values were
253 pooled, and statistical analysis was performed on the data (one-way ANOVA, followed by
254 an unpaired two-tailed student t-test). Scatter plots depict individual data points as well as
255 the median Golgi body displacement and corresponding standard deviation (SD) in μm .
256 The control lines (median = 1.14 μm , ranging from 0.13 to 4.95 μm) and full-length
257 AtCASP lines (median = 1.24 μm , ranging from 0.16 to 5.15 μm) did not significantly
258 differ from each other ($p = 0.7256$) (Figure 2d). Golgi displacement in mutant lines
259 (median = 0.67 μm , ranging from 0.08 to 4.24 μm) was reduced significantly compared to
260 both control ($p = 0.0184$) and full-length ($p = 0.0020$) lines. Similarly, as summarised in
261 Fig. 2e, the mean Golgi speed did not differ significantly between control (median = 0.61

262 μm , ranging from 0.08 to 1.7 μm , $p = 0.0740$) and full-length AtCASP (median = 0.57 μm ,
263 ranging from 0.07 to 2.11 μm) lines ($p = 0.5466$), but was significantly decreased in the
264 mutant (median = 0.34 μm , ranging from 0.05 to 1.61 μm) compared full-length lines ($p =$
265 0.0088).

266

267 *Optical trapping reveals that AtCASP is involved in tethering events at the Golgi-ER*
268 *interface*

269 Since Golgi movement parameters in the AtCASP lines were significantly different to the
270 control line, optical tweezers were used to physically probe whether these were due to
271 effecting the interaction with the ER. We hypothesised that if AtCASP had a role in
272 tethering Golgi bodies to the ER, any potential effects of mutant AtCASP- ΔCC over-
273 expression would become apparent upon manipulation of Golgi bodies with optical
274 tweezers *in planta*. The underlying physical principle of optical trapping is that a highly
275 focused laser beam is able to trap particles if they are a certain size (approx. 1 μm), and
276 their refractive index is different to that of their environment (Neuman and Block, 2004).
277 Golgi bodies fulfil these requirements, as their size is around 1 μm in diameter and due to
278 their condensed stack structure their refractive index differs from the surrounding
279 cytoplasm. In contrast, it has not been possible experimentally to trap ER membranes
280 (Sparkes *et al.*, 2009b).

281 Optical trapping was performed in *Arabidopsis* cotyledonary leaf epidermal cells of four to
282 five day old seedlings (before start of growth stage 1 and emergence of rosette leaves,
283 Boyes *et al.*, 2001), of mRFP-AtCASP- ΔACC /GFP-HDEL (n of cells = 10, n of Golgi
284 bodies = 45) and ST-mRFP/GFP-HDEL control lines (n of cells = 13, n of Golgi bodies =
285 53, Table 2). A new Golgi body was randomly chosen for every new trapping event. Leaf
286 samples were treated with the actin-depolymerising drug Latrunculin B before trapping, to
287 inhibit actin-based Golgi movement. Any subsequent movement was therefore due to the
288 physical micromanipulation of the trapped Golgi body, as the ER cannot be trapped
289 (Sparkes *et al.*, 2009b). In STmd-control cells, a trapping laser output of 70 mW was
290 required to trap Golgi bodies, and no trapping was possible with outputs below this. In
291 contrast, Golgi bodies in the AtCASP- ΔACC mutant line could easily be trapped with the

292 laser power set to 30 mW (Table 2). From the total number of Golgi bodies trapped in the
293 mutant line, 17 Golgi bodies moved just a few μm over the ER and then came to a halt,
294 whereas the rest could be moved over a longer distance across the cell. ER remodeling
295 along the tracks of trapped Golgi bodies occurred only in 15 instances in the mutant
296 (28%), compared to 41 instances in the control trapping events (91%). Sixteen Golgi
297 bodies in the mutant line detached from GFP-HDEL-labelled tubules during the trapping
298 event, and 11 of them re-attached to the ER as they were being moved. For the remaining
299 trapping events it was not possible to determine whether ER reattachment took place.

300 Figure 3a depicts movie frames from an optical trapping event in mutant AtCASP- ΔCC
301 cells (see Suppl. Movie 1). Turning the trapping laser on resulted in movement of a whole
302 group of Golgi bodies over a short distance (at time point 7.8 s). A single Golgi body
303 remained trapped (arrowhead), lost its ER tubule association and then moved freely
304 through the cell, until connection was re-established near an ER tubule upon release of the
305 optical trap (Fig. 3b, asterisk).

306 Surprisingly, in a few instances GFP-HDEL tubules appeared to follow Golgi bodies with
307 a significant gap after the connection had been disrupted, as shown in Figure 3b (and
308 Suppl. Movie 2). Movement of two Golgi bodies that were trapped simultaneously (Fig. 3b,
309 arrowhead) initially resulted in ER remodeling, until the connection broke (time point 7.8
310 s, asterisk). The ER tubule mirrored Golgi body movement with a delay (time points 11 s
311 to 16.8 s). From time point 20.4 s onwards, a second ER tubule mirrored Golgi body
312 movement (yellow arrowhead), appearing to attempt attachment to the trapped Golgi body.

313 Interestingly, the optical trapping data mirrored the observation made during the tracking
314 of Golgi bodies in cells expressing full-length mRPF-AtCASP, in which Golgi bodies
315 appeared to be 'sticky' and formed clusters or chains. In 64% of all trapping events
316 performed in full-length lines, two or more Golgi bodies were trapped and moved together,
317 in contrast to 35% in STtmd-mRFP and 47% in AtCASP- ΔCC lines (Fig. 4a, at similar
318 optical trapping force).

319 To test the degree of attachment in more detail, we used a TIRF-based optical trapping
320 system and captured Golgi bodies in control, full-length and mutant AtCASP *Arabidopsis*
321 cotyledons at similar trapping force range. For this experiment, 100 Golgi bodies in three

322 different leaves for each line (total $n = 300$) were randomly selected and scored as to
323 whether they could be manually trapped and moved, or not (Figure 4c). In STtmd-mRFP
324 cells, just 47% of Golgi bodies could be trapped, in cells expressing mRFP-AtCASP the
325 ability to trap Golgi bodies increased slightly to 57%. In contrast, in cells expressing
326 mRFP-AtCASP- Δ CC, we were able to trap 76% of Golgi bodies. Statistical analysis (one-
327 way ANOVA and unpaired two-tailed student t-test) showed that there was no significant
328 difference between the control and full-length AtCASP ($p=0.321$), but mRFP-AtCASP-
329 Δ CC differed significantly from the control ($p = 1.065 \times 10^{-8}$) and full-length mRFP-
330 AtCASP ($p = 2.091 \times 10^{-6}$).

331 Using ImageJ and the MTrackJ plugin, we mapped tracks of captured Golgi bodies in
332 relation to the tip of the remodelling ER tubule in STtmd-mRFP control lines (five tracks
333 in total, representative track shown in Fig. 5a), mRFP-AtCASP (six tracks, representative
334 track shown in Fig. 5b) and mRFP-AtCASP- Δ CC lines (21 tracks, Fig. 5c and d).
335 Arrowheads indicate trapped Golgi bodies. In control cells, Golgi body and ER tracks
336 overlaid almost perfectly with each other during micromanipulation (n of cells = 7, Fig. 5 a
337 and e, Suppl. Movie 3). Looking at tracks from cells expressing full length mRFP-AtCASP
338 ($n = 6$), we found that Golgi and ER tracks mirrored each other as they did in the control,
339 but the connection was more easily disrupted (Fig. 5 b and f, Suppl. Movie 4) compared to
340 the control. In cells expressing mRFP-AtCASP- Δ CC ($n = 6$), the instability of the ER-
341 Golgi connection was reflected in a non-uniform range of track patterns. For example, as
342 shown in Fig. 5 c and h (Suppl. Movie 5), an ER tubule initially followed a trapped Golgi
343 body (arrowhead) on the same trajectory. The connection was then lost (asterisk), but the
344 ER continued to mirror the Golgi body track but separated from each other by a distance
345 ranging from 0.6-1.6 μ m. In other instances, a captured Golgi body separated from the ER
346 (arrowhead, Fig. 5 d and h), would reconnect with the ER for the track length of a few
347 microns (asterisk) and break free again.

348 The gap width between the centre of the trapped Golgi body and the ER tubule tip in the
349 time series depicted in Fig. 5c varied throughout the optical trapping event. The distance
350 was measured in each of the nine frames in the movie. Values ranged between 0.62 μ m at
351 the beginning to 1.33 μ m at the end, with a mean width of 1.14 μ m.

352 We assessed the stability of the ER-Golgi connection per individual trapping time series in
353 control, full-length and mutant AtCASP lines (Fig. 6a) by calculating the ratio of frames
354 with an intact ER-Golgi connection versus the total frame number, working on the
355 assumption that trap movement was reasonably consistent over the short distances Golgi
356 bodies were moved. Thus, a ratio of 1 means that ER remodelling took place throughout
357 the whole trapping event, whereas a ratio of 0.5 indicates that the trapped Golgi body was
358 detached from the ER for half of the time series. In control cells, 95% of trapping events
359 showed a ratio of 1 (n=17), which reflects a stable ER-Golgi connection. In contrast, just
360 55% of trapped Golgi bodies in cells expressing mRFP-AtCASP (n=11), and 40% in
361 mRFP-AtCASP- Δ CC cells (n=15) retained a permanent connection to the ER throughout
362 the trapping event. The difference in length of disruption between the control and the full-
363 length ($p = 0.0031$) or mutant AtCASP ($p = 0.007$) lines was significant, as determined by
364 one-way ANOVA and unpaired two-tailed student-t test.

365 In control cells, only 10% of trapped Golgi bodies lost their ER connection, and if they
366 did, it occurred just once (Fig. 6b). In full-length AtCASP expressing cells, 60% of trapped
367 Golgi bodies detached from the ER once, which was significantly higher than control cells
368 (one-way ANOVA and unpaired two-tailed student t-test, $p = 0.0047$). The ER-Golgi
369 connection was most unstable in mRFP-AtCASP- Δ CC lines. In these, 40% of trapped
370 Golgi bodies detached and reattached to the ER more than once during one trapping event,
371 up to five times in one instance. This was significantly different to the control ($p = 0.012$),
372 but not significantly different to full-length AtCASP ($p = 0.356$).

373

374 **Discussion (1312 words)**

375 The advent of fluorescent protein technology permitted for the first time the observation of
376 the dynamics of plant Golgi stacks in living plant cells (Boevink *et al.*, 1998). The
377 movement of individual Golgi bodies over the cortical actin network whilst being
378 somehow attached to the ER was termed “stacks on tracks”. Subsequently it was shown
379 that transport of cargo between the ER was not dependent on the cytoskeleton (Brandizzi
380 *et al.*, 2002), that this association encompassed the protein components of the ER exit site
381 (da Silva *et al.*, 2004), and that the ER membrane itself was motile as well as Golgi bodies

382 (Runions *et al.*, 2006; Sparkes *et al.*, 2009b). However, it took the application of optical
383 trapping to conclusively demonstrate that the organelle-to-organelle adhesion at the ER-
384 Golgi body interface was sufficiently strong to permit remodelling of the tubular ER
385 network simply by moving Golgi bodies around in the cortex of leaf epidermal cells
386 (Sparkes *et al.*, 2009b). Here we show that overexpression of truncated AtCASP
387 (Latijnhouwers *et al.*, 2007; Renna *et al.*, 2005) interferes with ER-Golgi physical
388 interaction, showing that 1) ER and Golgi bodies are tethered rather than being
389 connections maintained through membranous extensions and 2) the ER-Golgi interface
390 may be organised by tethering proteins, the disturbance of one, AtCASP, resulting in an
391 alteration of Golgi movement and trapping properties.

392 *AtCASP functions as a tether between the ER and Golgi stack*

393 It could be predicted that if a protein is involved in tethering the Golgi stack to the ER,
394 then the parameters describing its movement with or over the ER may change upon its
395 disruption. Visually, this is difficult to assess from confocal time-lapse image series, other
396 than the observed clumping of Golgi stacks in *Arabidopsis* lines expressing full-length
397 mRFP-AtCASP. This clumping presumably occurs due to interactions between excess
398 coiled-coil domains on the Golgi surface. Quantitative image analysis revealed both a drop
399 in Golgi body velocity and reduction in their mean displacement in AtCASP- Δ CC
400 expressing cells, compared to non-clumped Golgi bodies in this AtCASP mutant or in
401 control ST-mRFP expressing cells. This could be interpreted either as interference with
402 putative motor protein activity at the ER Golgi interface or a loosening of the tethering at
403 the interface. If in this scenario the tether is loosened, then decoupling of the Golgi body
404 from its ER exit site supports the contention that Golgi movement is at least in part
405 generated via movement of the ER surface (Runions *et al.*, 2006), in which the exit site is
406 embedded. Alternatively, the movement of the Golgi attached to the ER exit site may affect
407 ER movement. It is still unclear to what extent the movement of ER and Golgi are
408 dependent upon one another, co-regulated events or mutually exclusive processes (Sparkes
409 *et al.* (Sparkes *et al.*, 2009a). To date there is little evidence for a Golgi-associated myosin
410 (Avisar *et al.*, 2009; Sparkes *et al.*, 2008), other than a study on the expression of a
411 truncated myosin, which occasionally labelled Golgi stacks (Li and Nebenfuhr, 2007).
412 Furthermore, the differences in the AtCASP- Δ CC mutant line were observed upon actin

413 depolymerisation during the trapping experiments. Therefore, it can be assumed that
414 interfering with tethering may be the most likely cause of the change in Golgi body
415 motility on expression of mutant AtCASP.

416 In this study, we utilised a more direct approach to probe Golgi tethering to the ER, which
417 was carried out on two different optical trapping set-ups, confocal and TIRF-based. Our
418 optical trapping data clearly demonstrates that interfering with the coiled-coil domain, and
419 thus with any tethering function, affects the physical Golgi-ER connection. We were able
420 to show that upon overexpression of the truncated AtCASP protein, the trap power
421 required to manipulate individual Golgi stacks was greatly reduced from that required for
422 wild type Golgi bodies marked with a different membrane construct. Presumably,
423 truncated AtCASP out-competed the native protein in a dominant-negative fashion. We
424 found that trapping of Golgi bodies in mutant lines was easier, and that the interface
425 between ER and Golgi could be disturbed under experimental conditions in which actin
426 had been depolymerised.

427

428 *AtCASP: One component of a larger tethering complex?*

429 In control Golgi-tagged plants, upon micromanipulation of Golgi bodies, the ER track
430 coincided almost perfectly with the Golgi track. Upon over expression of full-length
431 fluorescently tagged AtCASP, the connection appeared to be more easily disturbed than in
432 control cells, but the tracks of ER tips and Golgi bodies occasionally were able to mirror
433 each other. Golgi bodies still appeared to move on actin delimited 'tracks', but the
434 connection with the ER was loose. In cells expressing the deletion mutant, the disruption
435 of the putative tether was obvious. Golgi bodies broke free from the ER more easily than
436 in control STmd-mRFP or full-length mRFP-AtCASP expressing cells. Track patterns
437 were irregular and did not mirror that of the ER.

438 The gap observed on some occasions whilst being a micron plus between Golgi and ER,
439 showed the Golgi and ER following the same trajectory, suggests that AtCASP is not
440 solely responsible for tethering at the ER-Golgi interface, but might be part of a more
441 substantial tethering complex. Other components of such a complex might include other
442 *cis*-Golgi located golgins such as the plant homologue of the well-characterised tether
443 Atp115 (MAG4, Kang and Staehelin, 2008; Lerich *et al.*, 2012; Takahashi *et al.*, 2010), or

444 even the recently identified AtSec16/MAIGO5 (Takagi *et al.*, 2013). Gillingham and
445 colleagues (Gillingham *et al.*, 2002) reported an indirect interaction between the yeast
446 CASP homologue COY1 and the SNARE (Soluble N-ethylmaleimide-sensitive factor
447 Activating protein REceptor) protein Gos1p in yeast assays, as well as a small fraction of
448 COY1 co-precipitating with the COPII coat subunit hSec23 and Golgin-84. Another study
449 (Malsam *et al.*, 2005) identified mammalian CASP as component of an asymmetric
450 tethering complex, with CASP binding to Golgi membranes and interacting with Golgin84
451 on COPI vesicles, thus suggesting a role for CASP in retrograde transport. As many
452 protein functions within the secretory pathway are conserved between plants and
453 mammals, some interactions might be conserved as well, and we are currently analysing
454 potential AtCASP binding partners.

455

456 ***AtCASP as novel starting point to dissect the plant ER-Golgi interface***

457 Previous studies suggested a role for AtCASP in Golgi biogenesis, possibly as part of a
458 ‘platform’ that might act as base for the formation of early *cis*-Golgi structures (Ito *et al.*,
459 2012; Osterrieder *et al.*, 2010; Schoberer *et al.*, 2010). As immuno-labelling of GFP-
460 AtCASP located the construct to cisternal rims of Golgi stacks (Latijnhouwers *et al.*,
461 2007), AtCASP appears to be anchored through its transmembrane domain to *cis*-Golgi
462 membranes, while its coiled-coil domains (labelled by the N-terminal fluorophore) bind to
463 yet unidentified partners at the ER-Golgi interface. Triple labelling experiments with
464 fluorescent full-length and mutant fluorescent AtCASP versions, co-expressed with ER
465 exit site and COPII markers, as well as *cis*- or *trans*-Golgi membrane markers such as
466 glycosyltransferases (Schoberer and Strasser, 2011), could help to unravel the
467 subcompartmentalisation of key players at the plant ER-Golgi interface.

468 The biology of the ER-Golgi interface differs between plants and mammals in a variety of
469 aspects (Brandizzi and Barlowe, 2013). Based on this and on the results from our study, we
470 hypothesise that AtCASP could have different or additional functions in plants compared
471 to its animal and yeast homologues. Notably, the model of ER exit site organisation itself
472 is still in flux. The latest model, proposed by Glick (2014), replaces the concept of a
473 COPII-organising scaffold with that of a self-organising tethering framework, consisting of

474 ER exit sites (transitional ER sites in yeast), early Golgi membranes and tethering factors,
475 one of which might be CASP (Glick, 2014). Understanding the molecular make-up and
476 mechanisms of the plant ER-Golgi interface is crucial for our understanding of how
477 proteins pass through the secretory pathway. By identifying AtCASP as novel ER-Golgi
478 tether, we have gained a new entry point into the dissection of the plant ER-Golgi
479 interface.

480

481 ***Conclusion***

482 In conclusion this work indicates that leaf epidermal cell Golgi bodies are intimately
483 associated with the ER and that the connection is most likely maintained by a tethering
484 complex between the two organelles, thus not simply relying on membrane continuity
485 between the ER exit site and *cis*-Golgi membranes.

486

487 **Acknowledgements**

488 We thank Janet Evins for help with growing plants. The work was supported by a BBSRC
489 grant (BB/J000302/1) and a Royal Society Travel grant to CH .

490

491 **Short legends for supporting information (separate files)**

492 **Suppl. Movie 1:**

493 Confocal images of a timeseries, taken over 34.4 seconds, showing *Arabidopsis thaliana*
494 leaf epidermal cells with endoplasmic reticulum labelled with GFP-HDEL and Golgi
495 bodies labelled with mRFP- AtCASP- Δ CC. Initially, a whole group of Golgi bodies moved
496 with the trap. A single Golgi body remained in the trap, lost connection to the ER tubule,
497 and then moved freely through the cell until connection was re-established near an ER
498 tubule. Scale bar = 2 μ m.

499

500 **Suppl. Movie 2:**

501 Confocal images of a timeseries, taken over 70.4 seconds, showing *Arabidopsis thaliana*
502 leaf epidermal cells with the endoplasmic reticulum labelled with GFP-HDEL, and Golgi
503 bodies labelled with mRFP-AtCASP- Δ CC. The optically trapped Golgi body lost its
504 connection to the ER, its movement being mirrored by the ER with a gap between the
505 both. Scale bar = 2 μ m.

506 **Suppl. Movie 3:**

507 Confocal images of a timeseries, taken over 15.24 seconds, showing *Arabidopsis thaliana*
508 leaf epidermal cells with the endoplasmic reticulum labelled with GFP-HDEL and Golgi
509 bodies labelled with STmd-mRFP. The movement of the trapped Golgi body and the tip of
510 the ER tubule overlaid almost perfectly with each other during micromanipulation. Scale
511 bar = 2 μ m.

512 **Suppl. Movie 4:**

513 Confocal images of a timeseries, taken over 10.40 seconds, showing *Arabidopsis thaliana*
514 leaf epidermal cells with the endoplasmic reticulum labelled with GFP-HDEL and Golgi
515 bodies labelled with mRFP-AtCASP. Golgi and ER tubule tracks mirrored each other as in
516 the control, but the ER-Golgi connection was more easily disrupted. Scale bar = 2 μ m.

517 **Suppl. Movie 5:**

518 Confocal images of a timeseries, taken over 10.27 seconds, showing *Arabidopsis thaliana*
519 leaf epidermal cells with endoplasmic reticulum labelled with GFP-HDEL and Golgi
520 bodies labelled with mRFP-AtCASP- Δ CC. The ER tubule initially followed the trapped
521 Golgi body. The connection became disrupted, but the ER continued to mirror the Golgi
522 body movement. Scale bar = 2 μ m.

523

524

525 **Table 1.** Numbers of *Arabidopsis* lines, cells and Golgi bodies used for analysis of velocity
 526 and displacement.

Line	Independent lines	Individual plants per line	Repetitions per line	Total n of cells	Total n of Golgi bodies
STtmd-mRFP/GFP-HDEL	1	5	3	41	332
mRFP-AtCASP/GFP-HDEL	2	7 and 4	3 and 2	46 32	388 240
mRFP-AtCASP- Δ CC/GFP-HDEL	2	6 and 4	3 and 2	43 23	456 174

527

528 **Table 2.** The effects of optical trapping in control and AtCASP mutant *Arabidopsis* leaf
 529 epidermal cells.

	Control	AtCASP- Δ CC
Laser power [mW] required for Golgi body trapping	70	30-40
Number of analysed cells	10	13
Total number of trapped Golgi bodies	45	53
Number of Golgi bodies trapped and ER remodelling follows Golgi tracks	41	15
ER-Golgi connection disrupted	3	16
Number of instances in which ER tubule movement mirrored movement of a trapped Golgi body, with a visible gap between Golgi body and ER tubule tip	0	4

530

531

532 **Figure legends (1070 words)**

533

534

535 **Figure 1 Fluorescent AtCASP full-length and mutant constructs**

536 a) Diagram depicting the domain structure of fluorescent AtCASP constructs used in this
537 study: full-length AtCASP and a truncation AtCASP- Δ CC consisting of its C-terminus
538 (463 base pairs including the transmembrane domain), but missing the coiled-coil domains
539 which convey its tethering function. CC = coiled-coil domain, TMD = transmembrane
540 domain, mRFP = monomeric red fluorescent protein.

541 b) and c) Confocal laser scanning micrographs of tobacco leaf epidermal cells three days
542 after transfection, transiently expressing the standard Golgi marker STtmd-GFP (green)
543 and b) full-length mRFP-AtCASP or c) of mRFP-AtCASP- Δ CC (magenta). Both
544 constructs co-locate in punctate structures which represent Golgi bodies. Cells were
545 transfected using agrobacterium-mediated transformation. STtmd-GFP was infiltrated at
546 OD₆₀₀ = 0.05, mRFP-AtCASP constructs at OD₆₀₀ = 0.1. Scale bars = 20 μ m.

547

548 **Figure 2 Live-cell imaging and quantitative analysis of Golgi body dynamics in**
549 **AtCASP full-length and mutant *Arabidopsis thaliana* lines.**

550 a) - c) Confocal laser scanning micrographs of *Arabidopsis* cotyledonary leaf cells stably
551 expressing the endoplasmic reticulum (ER) marker GFP-HDEL (green) and a) STtmd-
552 mRFP, b) mRFP-AtCASP or c) mRFP-AtCASP- Δ CC (magenta). No obvious differences
553 in Golgi body morphology, location or dynamics could be observed through qualitative
554 live-cell imaging. Scale bars = 5 μ m.

555 d) – e) Quantitative analysis of d) mean speed and e) mean displacement of fluorescently
556 labelled Golgi bodies in stable *Arabidopsis* lines expressing either the control STtmd-
557 mRFP, mRFP-AtCASP, or mRFP-AtCASP- Δ CC. The mean speed and displacement of
558 individual Golgi bodies were determined manually using the Fiji particle tracking plugin
559 MtrackJ (Meijering et al. 2012). Mean speed and displacement values per cell were
560 calculated from pooled Golgi body values (n of Golgi bodies per video ranged between 3-
561 17). Statistical tests (one-way ANOVA and unpaired two-tailed student t-test) were then

562 performed on the pooled cell values (n of cells STtmd =41, AtCASP-FL = 79, AtCASP-
563 Δ CC = 63, see Table 1 for full summary). Scatter plots depict the mean as horizontal bar,
564 error bars depict the SD. Asterisks represent the level of significance (* p <0.05 , ** p= <
565 0.01).

566

567 **Figure 3 Disruption of the ER-Golgi connection in mutant AtCASP- Δ CC cells.**

568 Confocal images showing still images of a time series over 34.4 seconds during optical
569 trapping of Golgi bodies in transgenic *Arabidopsis* cotyledonary leaf epidermal cells.
570 Plants were expressing mRFP-AtCASP- Δ CC (magenta) and the ER marker GFP-HDEL
571 (green). Arrowheads point to optically trapped Golgi bodies. Scale bars = 2 μ m. (a)
572 Several Golgi bodies moved with the trap across a short distance. A single Golgi body
573 remained in the trap and moved through the cell detached from the ER. (b) A Golgi body
574 was trapped and the ER-Golgi connection was disrupted at time point 7.8 s (asterisk). The
575 ER tubule followed the Golgi body with a gap. At time point 20.4 s, a second ER tubule
576 mirrored Golgi body movement with a similar gap (arrowhead).

577

578 **Figure 4 Comparing the ability to trap Golgi bodies in STtmd-mRFP control, full-
579 length mRFP-AtCASP and mutant mRFP-AtCASP- Δ CC lines.**

580 a) Two or more Golgi bodies were captured in 64% of trapping events in full-length
581 AtCASP lines, compared to just 35% in control, and 47% in AtCASP- Δ CC lines.
582 Expression of full-length mRFP-AtCASP appears to make Golgi bodies ‘stickier’.

583 b) Average numbers of three experiments (total n=300) of trapping control, full-length and
584 mutant AtCASP Golgi bodies in *Arabidopsis* cotyledons using a TIRF-Tweezer system.
585 Compared to 46% trapped Golgi bodies control cells and 57% trapped Golgi in mRFP-
586 AtCASP cells, 76% of Golgi bodies expressing the truncation could be trapped. The
587 STtmd control and AtCASP full-length line did not significantly differ from each other
588 (Chi-square test, p = 0.321), but the AtCASP- Δ CC line differed significantly from the
589 control (p=1.065x10⁻⁸) and the full-length line (p=2.091x10⁻⁶).

590 **Figure 5 ER and Golgi body tracks differ between control and mutant lines**

591 (a-d) Confocal images showing the effect of optically trapping individual Golgi bodies in
592 *Arabidopsis* cotyledons expressing GFP-HDEL (shown in green) and (a) the control
593 marker STtmd-mRFP, (b) full-length GFP-AtCASP or (c-d) truncated GFP-AtCASP- Δ CC
594 (all shown in magenta). (e-h) Visualisation of Golgi body tracks (magenta) in relation to
595 the ER tubule tip (green). Arrowheads indicate trapped Golgi bodies. Scale bars = 2 μ m.

596 (a) and (e) Control cell expressing STtmd-mRFP and GFP-HDEL. The Golgi-ER
597 connection remained intact and both tracks were closely associated. (b) and (f) Cell
598 expressing mRFP-AtCASP and GFP-HDEL. Golgi and ER remained connected only for a
599 short time before the connection was disrupted (asterisk). (c) and (g) Cell expressing
600 mRFP-AtCASP- Δ CC and GFP-HDEL. ER and Golgi moved together for the first part of
601 the time series. The connection then broke apart (asterisk) and the ER followed the Golgi
602 body with a gap. (d) and (h) Time series showing an example in which the ER-Golgi
603 connection was disrupted immediately after trapping. A second ER tubule unsuccessfully
604 attempted to reconnect with the Golgi body (asterisk).

605

606 **Figure 6 Semi-quantitative analysis of Golgi body trapping in control and AtCASP**
607 **full-length and mutant expressing *Arabidopsis* lines**

608 Assessing the stability of the connection between individual Golgi bodies and the ER in
609 *Arabidopsis* cotyledonary leaf epidermal cells expressing STtmd-mRFP/GFP-HDEL
610 (control, n=17), full-length mRFP-AtCASP/GFP-HDEL (n=11) or truncated mRFP-
611 AtCASP- Δ CC/GFP-HDEL (n=15). Errors bars depict means and standard deviations.

612 a) Scatterplot displaying the ratio of number of frames per trapping event with an intact
613 ER-Golgi connection versus the number of total frames. A ratio of 1 indicates an intact
614 connection over the whole duration of the time series. The smaller the ratio, the longer the
615 connection was disrupted during a time series. The ER-Golgi connection was disrupted
616 significantly longer in cells expressing mRFP-AtCASP ($p = 0.0031$) or mRFP-AtCASP-
617 Δ CC ($p = 0.007$), compared to control cells. Full-length and mutant AtCASP lines did not
618 differ significantly ($p = 0.75$).

619 b) Scatterplot showing the number times that the ER-Golgi connection was disrupted per
620 individual trapping event. In almost all of the trapping events in control cells, the
621 connection remained intact. Its instability (symbolised by repeated detachments and
622 reattachments of the trapped Golgi body with the ER) increased significantly in mRFP-
623 AtCASP cells ($p = 0.0047$) and mRFP-AtCASP- Δ CC cells ($p = 0.012$). No significant
624 difference was observed between full-length and mutant AtCASP ($p = 0.356$).

References

- Altan-Bonnet N, Sougrat R, Lippincott-Schwartz J.** 2004. Molecular basis for Golgi maintenance and biogenesis. *Current Opinion in Cell Biology* **16**, 364-372.
- Avisar D, Abu-Abied M, Belausov E, Sadot E, Hawes C, Sparkes IA.** 2009. A comparative study of the involvement of 17 Arabidopsis myosin family members on the motility of Golgi and other organelles. *Plant Physiology* **150**, 700-709.
- Barinaga-Rementeria Ramirez I, Lowe M.** 2009. Golgins and GRASPs: Holding the Golgi together. *Seminars in Cell & Developmental Biology* **20**, 770-779.
- Barr FA, Short B.** 2003. Golgins in the structure and dynamics of the Golgi apparatus. *Current Opinion in Cell Biology* **15**, 405-413.
- Boevink P, Oparka K, Santa Cruz S, Martin B, Betteridge A, Hawes C.** 1998. Stacks on tracks: the plant Golgi apparatus traffics on an actin/ER network. *Plant Journal* **15**, 441-447.
- Boyes DC, Zayed AM, Ascenzi R, McCaskill AJ, Hoffman NE, Davis KR, Gortlach J.** 2001. Growth stage-based phenotypic analysis of Arabidopsis: a model for high throughput functional genomics in plants. *Plant Cell* **13**, 1499-1510.
- Brandizzi F, Barlowe C.** 2013. Organization of the ER-Golgi interface for membrane traffic control. *Nature Reviews: Molecular Cell Biology* **14**, 382-392.
- Brandizzi F, Snapp EL, Roberts AG, Lippincott-Schwartz J, Hawes C.** 2002. Membrane protein transport between the endoplasmic reticulum and the Golgi in tobacco leaves is energy dependent but cytoskeleton independent: evidence from selective photobleaching. *Plant Cell* **14**, 1293-1309.
- Chia PZ, Gleeson PA.** 2014. Membrane tethering. *F1000Prime Rep* **6**, 74.
- Clough SJ, Bent AF.** 1998. Floral dip: a simplified method for *Agrobacterium*-mediated transformation of *Arabidopsis thaliana*. *Plant Journal* **16**, 735-743.
- da Silva LL, Snapp EL, Denecke J, Lippincott-Schwartz J, Hawes C, Brandizzi F.** 2004. Endoplasmic reticulum export sites and Golgi bodies behave as single mobile secretory units in plant cells. *Plant Cell* **16**, 1753-1771.
- Foresti O, Denecke J.** 2008. Intermediate organelles of the plant secretory pathway: identity and function. *Traffic* **9**, 1599-1612.
- Gao H, Metz J, Teanby NA, Ward AD, Botchway SW, Coles B, Pollard MR, Sparkes I.** 2016. In Vivo Quantification of Peroxisome Tethering to Chloroplasts in Tobacco Epidermal Cells Using Optical Tweezers. *Plant Physiology* **170**, 263-272.

- Gillingham AK, Munro S.** 2003. Long coiled-coil proteins and membrane traffic. *Biochimica et Biophysica Acta* **1641**, 71-85.
- Gillingham AK, Pfeifer AC, Munro S.** 2002. CASP, the alternatively spliced product of the gene encoding the CCAAT-displacement protein transcription factor, is a Golgi membrane protein related to giantin. *Molecular Biology of the Cell* **13**, 3761-3774.
- Gilson PR, Vergara CE, Kjer-Nielsen L, Teasdale RD, Bacic A, Gleeson PA.** 2004. Identification of a Golgi-localised GRIP domain protein from *Arabidopsis thaliana*. *Planta* **219**, 1050-1056.
- Glick BS.** 2014. Integrated self-organization of transitional ER and early Golgi compartments. *Bioessays* **36**, 129-133.
- Hanton SL, Matheson LA, Chatre L, Brandizzi F.** 2009. Dynamic organization of COPII coat proteins at endoplasmic reticulum export sites in plant cells. *Plant Journal* **57**, 963-974.
- Hanton SL, Renna L, Bortolotti LE, Chatre L, Stefano G, Brandizzi F.** 2005. Diacidic motifs influence the export of transmembrane proteins from the endoplasmic reticulum in plant cells. *Plant Cell* **17**, 3081-3093.
- Hawes C, Osterrieder A, Hummel E, Sparkes I.** 2008. The plant ER-Golgi interface. *Traffic* **9**, 1571-1580.
- Hawes C, Satiat-Jeunemaitre B.** 2005. The plant Golgi apparatus-going with the flow. *Biochimica et Biophysica Acta* **1744**, 466-480.
- Hawes C, Schoberer J, Hummel E, Osterrieder A.** 2010. Biogenesis of the plant Golgi apparatus. *Biochemical Society Transactions* **38**, 761-767.
- Ito Y, Uemura T, Shoda K, Fujimoto M, Ueda T, Nakano A.** 2012. *cis*-Golgi proteins accumulate near the ER exit sites and act as the scaffold for Golgi regeneration after brefeldin A treatment in tobacco BY-2 cells. *Molecular Biology of the Cell* **23**, 3203-3214.
- Kang BH, Staehelin LA.** 2008. ER-to-Golgi transport by COPII vesicles in *Arabidopsis* involves a ribosome-excluding scaffold that is transferred with the vesicles to the Golgi matrix. *Protoplasma* **234**, 51-64.
- Karimi M, Inze D, Depicker A.** 2002. GATEWAY vectors for *Agrobacterium*-mediated plant transformation. *Trends in Plant Science* **7**, 193-195.
- Klumperman J.** 2011. Architecture of the mammalian Golgi. *Cold Spring Harbour Perspectives in Biology* **3**.
- Latijnhouwers M, Gillespie T, Boevink P, Kriechbaumer V, Hawes C, Carvalho CM.** 2007. Localization and domain characterization of *Arabidopsis* golgin candidates. *Journal of Experimental Botany* **58**, 4373-4386.

Latijnhouwers M, Hawes C, Carvalho C. 2005a. Holding it all together? Candidate proteins for the plant Golgi matrix. *Current Opinion in Plant Biology* **8**, 632-639.

Latijnhouwers M, Hawes C, Carvalho C, Oparka K, Gillingham AK, Boevink P. 2005b. An *Arabidopsis* GRIP domain protein locates to the *trans*-Golgi and binds the small GTPase ARL1. *Plant Journal* **44**, 459-470.

Lerich A, Hillmer S, Langhans M, Scheuring D, van Bentum P, Robinson DG. 2012. ER import sites and their relationship to ER exit sites: A new model for bidirectional ER-Golgi transport in higher plants. *Frontiers in Plant Science* **3**, 143.

Li JF, Nebenfuhr A. 2007. Organelle targeting of myosin XI is mediated by two globular tail subdomains with separate cargo binding sites. *Journal of Biological Chemistry* **282**, 20593-20602.

Lievens PM, Tufarelli C, Donady JJ, Stagg A, Neufeld EJ. 1997. CASP, a novel, highly conserved alternative-splicing product of the CDP/cut/cux gene, lacks cut-repeat and homeo DNA-binding domains, and interacts with full-length CDP in vitro. *Gene* **197**, 73-81.

Lorente-Rodriguez A, Barlowe C. 2011. Entry and exit mechanisms at the *cis*-face of the Golgi complex. *Cold Spring Harbour Perspectives in Biology* **3**.

Malsam J, Satoh A, Pelletier L, Warren G. 2005. Golgin tethers define subpopulations of COPI vesicles. *Science* **307**, 1095-1098.

Malsam J, Söllner TH. 2011. Organization of SNAREs within the Golgi Stack. *Cold Spring Harbor Perspectives in Biology* **3**, a005249.

Matheson LA, Hanton SL, Rossi M, Latijnhouwers M, Stefano G, Renna L, Brandizzi F. 2007. Multiple roles of ADP-ribosylation factor 1 in plant cells include spatially regulated recruitment of coatamer and elements of the Golgi matrix. *Plant Physiology* **143**, 1615-1627.

Meijering E, Dzyubachyk O, Smal I. 2012. Methods for cell and particle tracking. *Methods in Enzymology* **504**, 183-200.

Nakamura N, Wei JH, Seemann J. 2012. Modular organization of the mammalian Golgi apparatus. *Current Opinion in Cell Biology* **24**, 467-474.

Nebenführ A, Gallagher LA, Dunahay TG, Frohlick JA, Mazurkiewicz AM, Meehl JB, Staehelin LA. 1999. Stop-and-go movements of plant Golgi stacks are mediated by the acto-myosin system. *Plant Physiology* **121**, 1127-1142.

Neuman KC, Block SM. 2004. Optical trapping. *Review of Scientific Instruments* **75**, 2787-2809.

Osterrieder A. 2012. Tales of tethers and tentacles: golgins in plants. *Journal of Microscopy* **247**, 68-77.

- Osterrieder A, Hummel E, Carvalho CM, Hawes C.** 2010. Golgi membrane dynamics after induction of a dominant-negative mutant Sar1 GTPase in tobacco. *Journal of Experimental Botany* **61**, 405-422.
- Park M, Jürgens G.** 2011. Membrane traffic and fusion at post-Golgi compartments. *Frontiers in Plant Science* **2**, 111.
- Polishchuk RS, Mironov AA.** 2004. Structural aspects of Golgi function. *Cellular and Molecular Life Sciences* **61**, 146-158.
- Renna L, Hanton SL, Stefano G, Bortolotti L, Misra V, Brandizzi F.** 2005. Identification and characterization of AtCASP, a plant transmembrane Golgi matrix protein. *Plant Molecular Biology* **58**, 109-122.
- Robinson DG, Brandizzi F, Hawes C, Nakano A.** 2015. Vesicles versus tubes: Is endoplasmic reticulum-Golgi transport in plants fundamentally different from other eukaryotes? *Plant Physiology* **168**, 393-406.
- Robinson DG, Herranz M-C, Bubeck J, Pepperkok R, Ritzenthaler C.** 2007. Membrane dynamics in the early secretory pathway. *Critical Reviews in Plant Sciences* **26**, 199 - 225.
- Runions J, Brach T, Kuhner S, Hawes C.** 2006. Photoactivation of GFP reveals protein dynamics within the endoplasmic reticulum membrane. *Journal of Experimental Botany* **57**, 43-50.
- Sambrook J, W. RD.** 2001. *Molecular cloning - a laboratory manual*. Cold Spring Harbor: Cold Spring Harbor Laboratory Press.
- Schindelin J, Arganda-Carreras I, Frise E, Kaynig V, Longair M, Pietzsch T, Preibisch S, Rueden C, Saalfeld S, Schmid B, Tinevez J-Y, White DJ, Hartenstein V, Eliceiri K, Tomancak P, Cardona A.** 2012. Fiji: an open-source platform for biological-image analysis. *Nature Methods* **9**, 676-682.
- Schoberer J, Runions J, Steinkellner H, Strasser R, Hawes C, Osterrieder A.** 2010. Sequential depletion and acquisition of proteins during Golgi stack disassembly and reformation. *Traffic* **11**, 1429-1444.
- Schoberer J, Strasser R.** 2011. Sub-compartmental organization of Golgi-resident N-glycan processing enzymes in plants. *Mol Plant* **4**, 220-228.
- Short B, Haas A, Barr FA.** 2005. Golgins and GTPases, giving identity and structure to the Golgi apparatus. *Biochimica et Biophysica Acta (BBA) - Reviews on Cancer* **1744**, 383-395.
- Sparkes I.** 2016. Using optical tweezers to characterize physical tethers at membrane contact sites: Grab it, pull it, set it free? *Frontiers in Cell and Developmental Biology* **4**, 22.

Sparkes I, Runions J, Hawes C, Griffing L. 2009a. Movement and remodeling of the endoplasmic reticulum in nondividing cells of tobacco leaves. *Plant Cell* **21**, 3937-3949.

Sparkes IA. 2010. Motoring around the plant cell: insights from plant myosins. *Biochemical Society Transactions* **38**, 833-838.

Sparkes IA, Ketelaar T, De Ruijter NCA, Hawes C. 2009b. Grab a Golgi: Laser trapping of Golgi bodies reveals *in vivo* interactions with the endoplasmic reticulum. *Traffic* **10**, 567-571.

Sparkes IA, Runions J, Kearns A, Hawes C. 2006. Rapid, transient expression of fluorescent fusion proteins in tobacco plants and generation of stably transformed plants. *Nature Protocols* **1**, 2019-2025.

Sparkes IA, Teanby NA, Hawes C. 2008. Truncated myosin XI tail fusions inhibit peroxisome, Golgi, and mitochondrial movement in tobacco leaf epidermal cells: a genetic tool for the next generation. *Journal of Experimental Botany* **59**, 2499-2512.

Staehelein LA, Moore I. 1995. The plant Golgi apparatus: Structure, functional organization and trafficking mechanisms. *Annual Review of Plant Physiology and Plant Molecular Biology* **46**, 261-288.

Takagi J, Renna L, Takahashi H, Koumoto Y, Tamura K, Stefano G, Fukao Y, Kondo M, Nishimura M, Shimada T, Brandizzi F, Hara-Nishimura I. 2013. MAIGO5 functions in protein export from Golgi-associated endoplasmic reticulum exit sites in *Arabidopsis*. *Plant Cell* **25**, 4658-4675.

Takahashi H, Tamura K, Takagi J, Koumoto Y, Hara-Nishimura I, Shimada T. 2010. MAG4/Atp115 is a Golgi-localized tethering factor that mediates efficient anterograde transport in *Arabidopsis*. *Plant & Cell Physiology* **51**, 1777-1787.

Wang Y, Seemann J. 2011. Golgi biogenesis. *Cold Spring Harbour Perspectives in Biology* **3**, a005330.

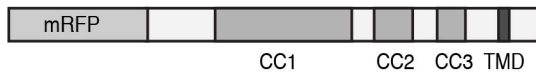
Wilson C, Ragnini-Wilson A. 2010. Conserved molecular mechanisms underlying homeostasis of the Golgi complex. *International Journal of Cell Biology* **2010**.

Wong M, Munro S. 2014. Membrane trafficking. The specificity of vesicle traffic to the Golgi is encoded in the golgin coiled-coil proteins. *Science* **346**, 1256898.

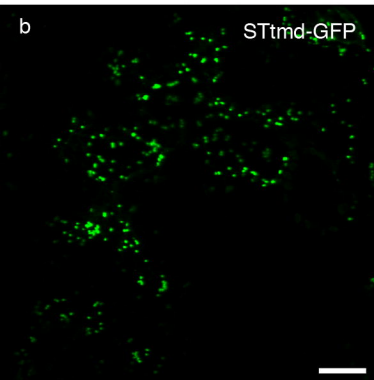
Zheng H, Kunst L, Hawes C, Moore I. 2004. A GFP-based assay reveals a role for RHD3 in transport between the endoplasmic reticulum and Golgi apparatus. *Plant Journal* **37**, 398-414.

a

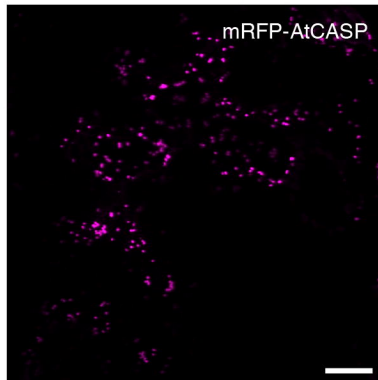
mRFP-AtCASP

mRFP-AtCASP- Δ CC**b**

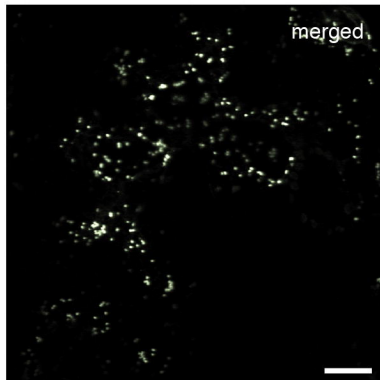
STtmd-GFP



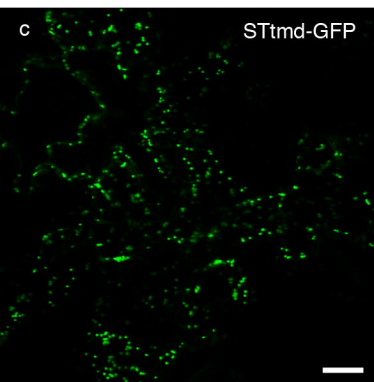
mRFP-AtCASP



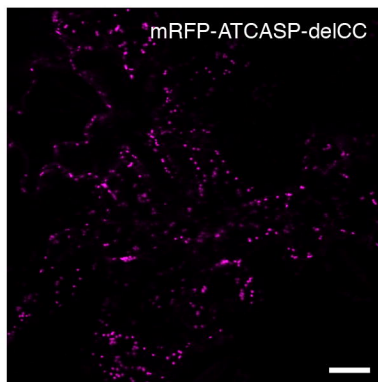
merged

**c**

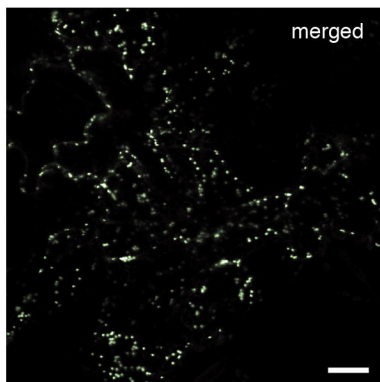
STtmd-GFP

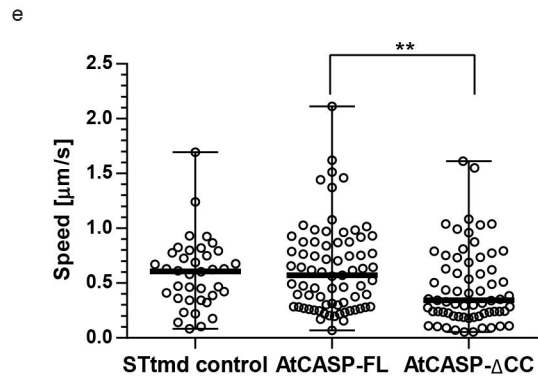
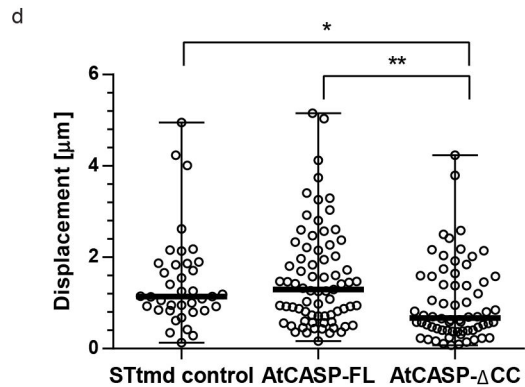
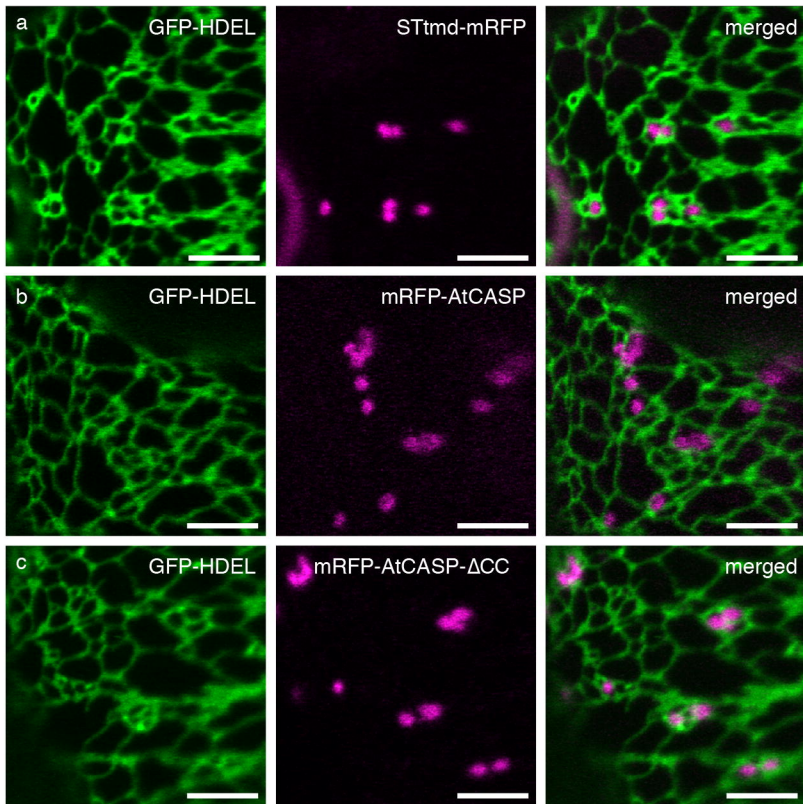


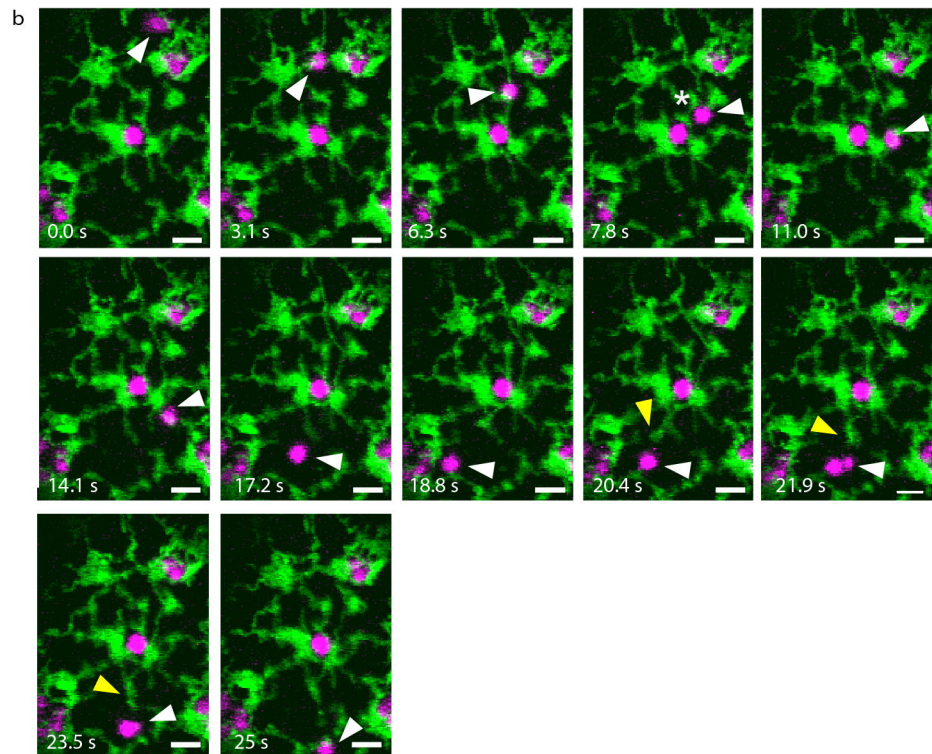
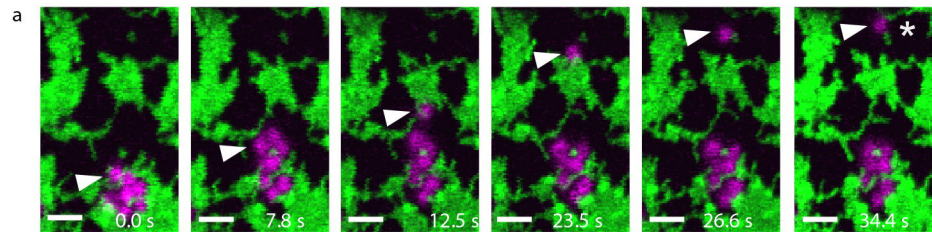
mRFP-ATCASP-delCC



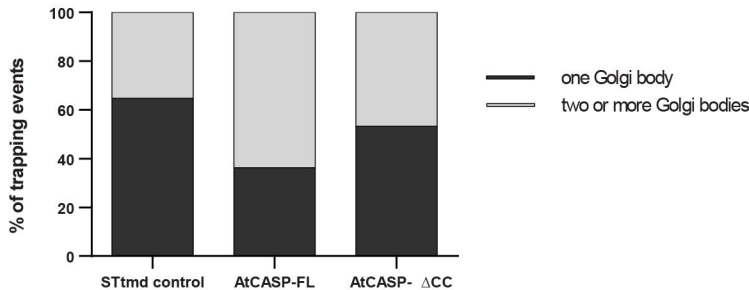
merged



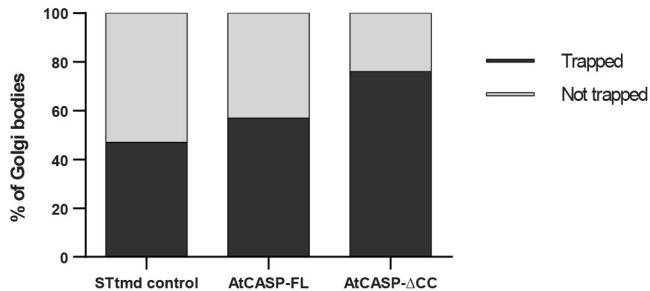


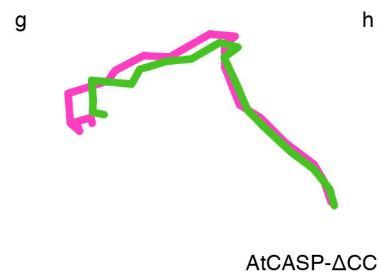
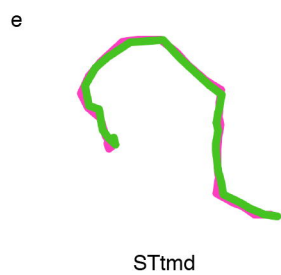
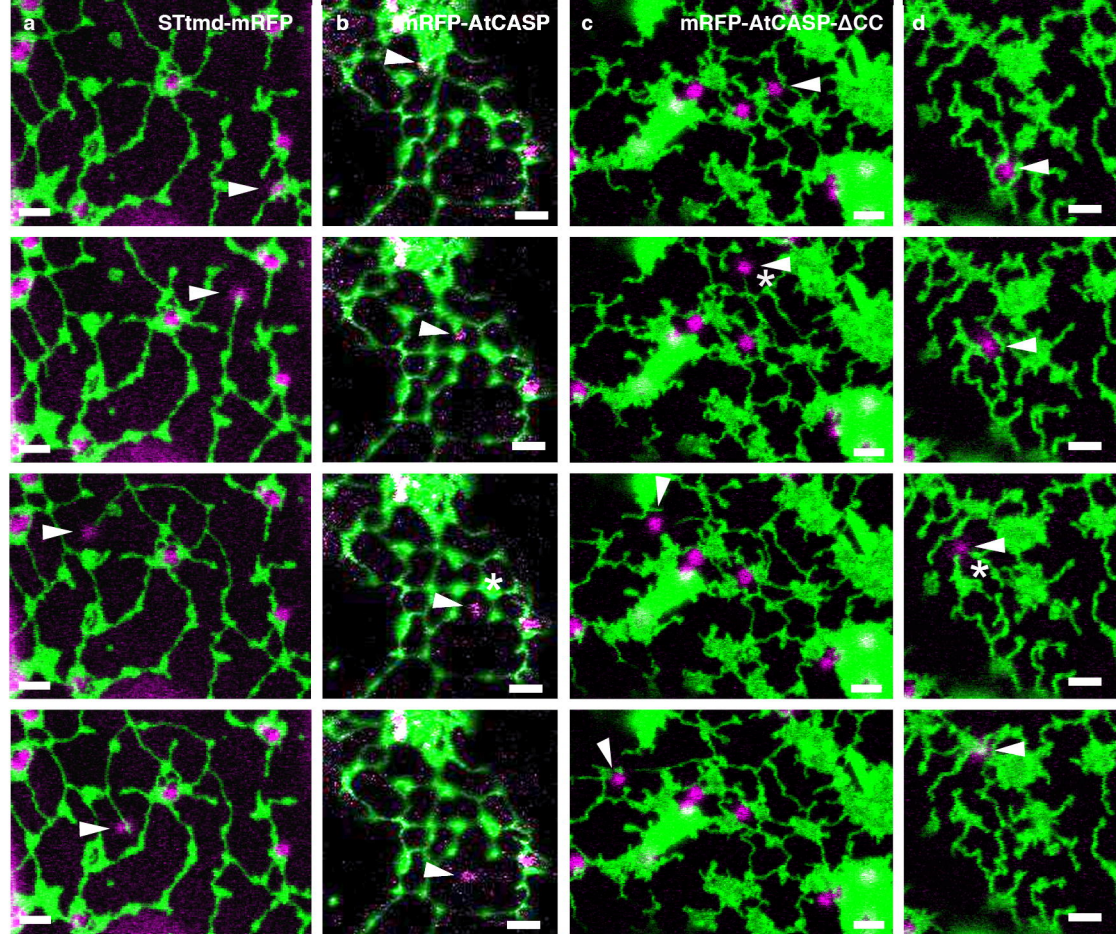


a



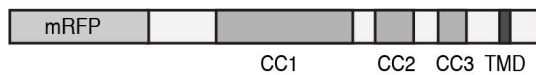
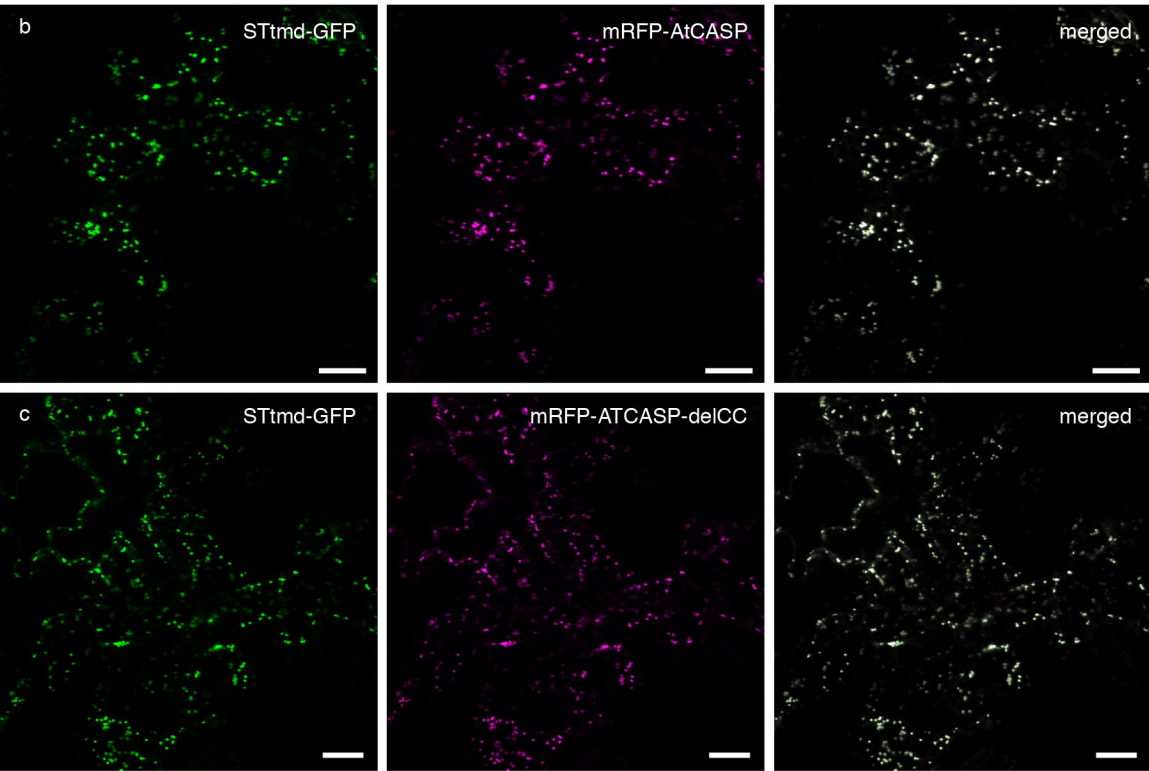
b

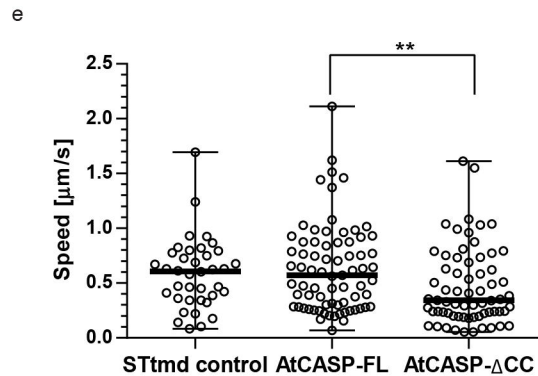
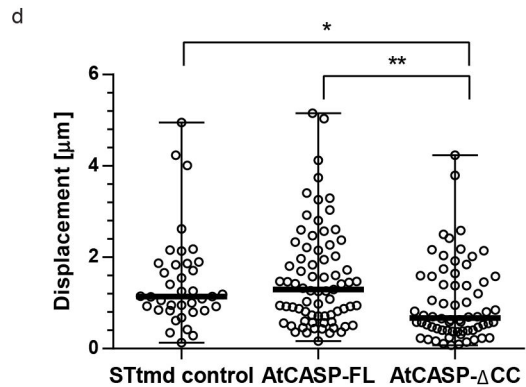
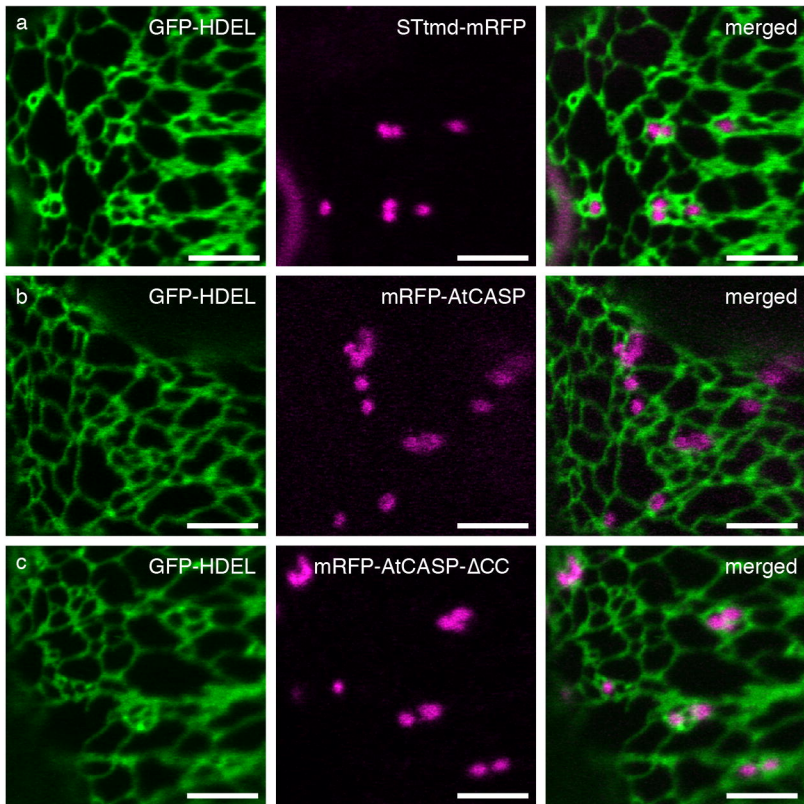


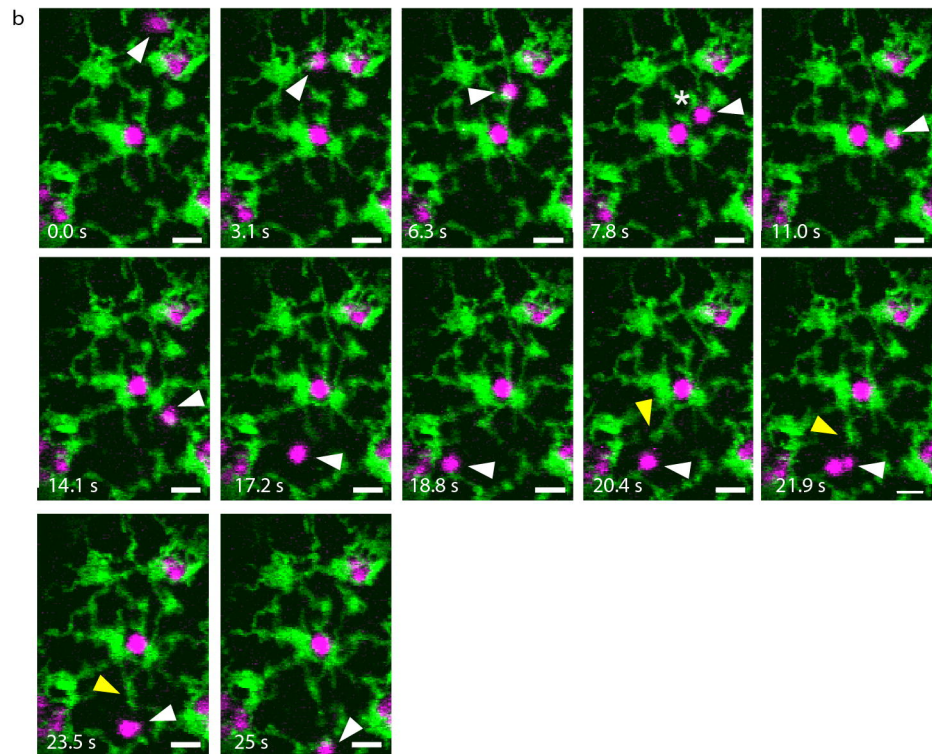
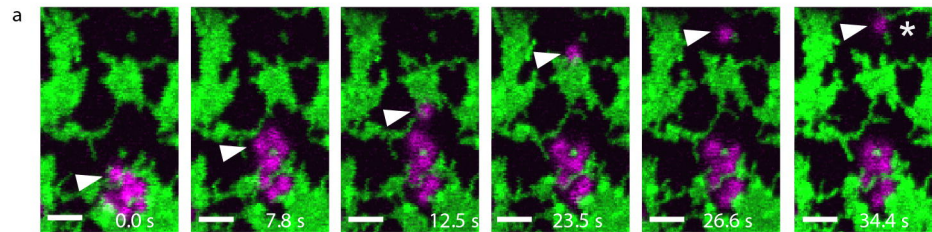


a

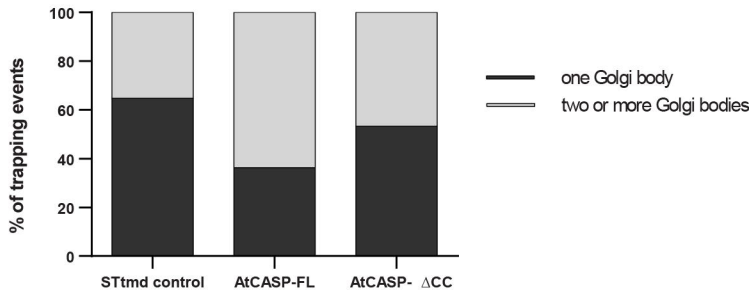
mRFP-AtCASP

mRFP-AtCASP- Δ CC

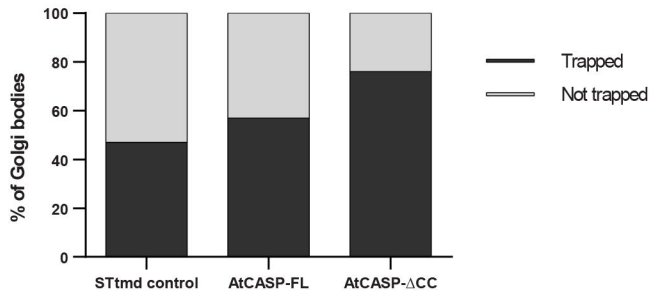


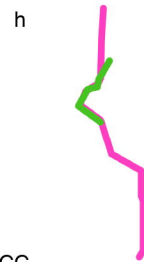
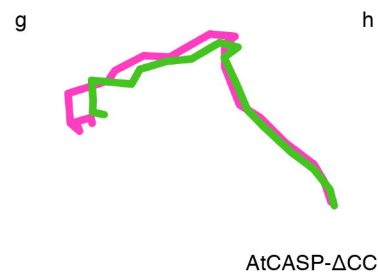
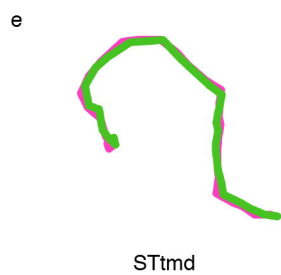
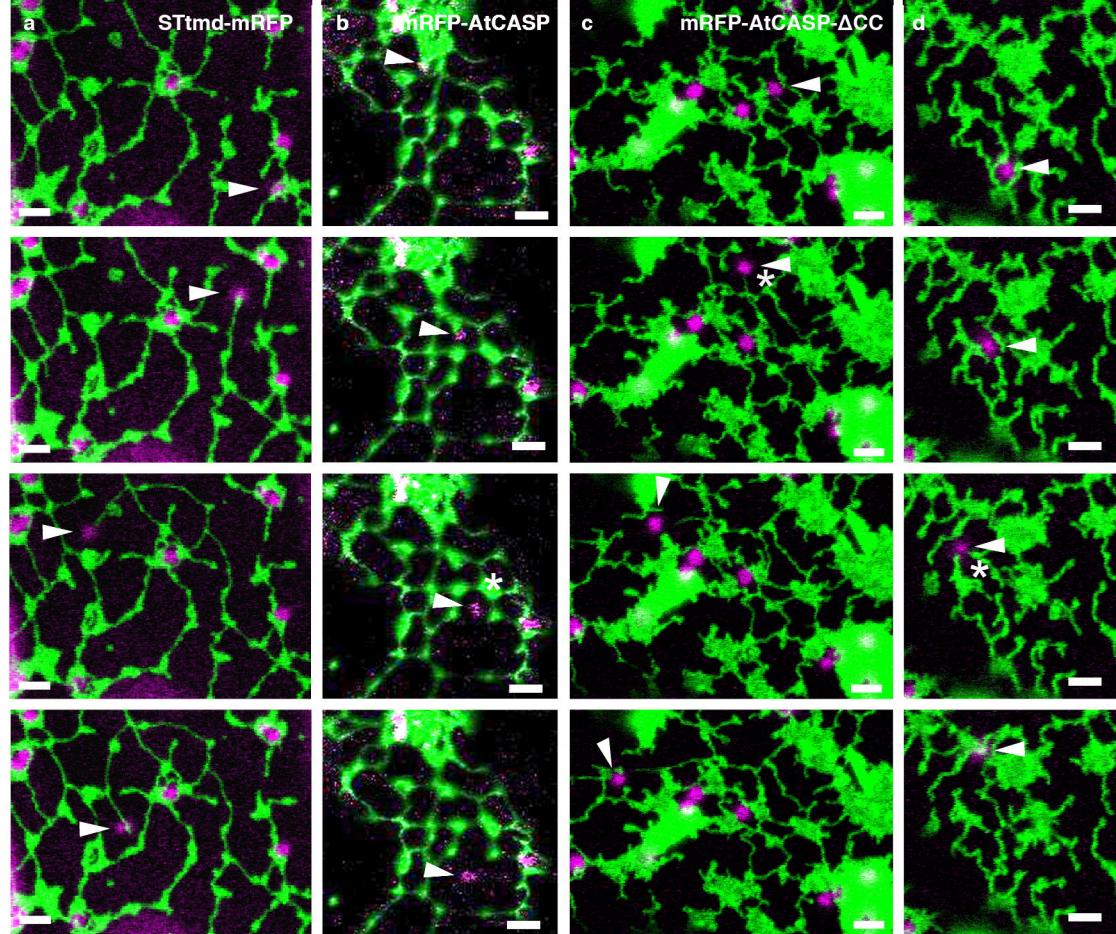


a

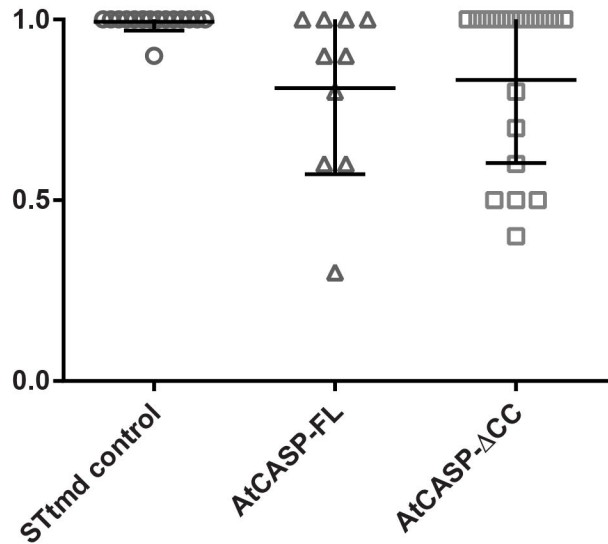


b





a



b

